Supporting Information

Design of 3*d* Transition Metal Embedded Asymmetric HMo_2CF for N_2 Electrocatalytic Conversion to NH_3

Lu Deng[a,b], Fei Wu[a,b], Wanbin Guan*[b,c], Zhiyi Lu[b,c], Qiuju Zhang*[b,c]

[a] School of Materials Science & Chemical Engineering, Ningbo University, Ningbo, Zhejiang 315211, P. R. China

[b] Zhejiang Key Laboratory of Advanced Fuel Cells and Electrolyzers Technology, Ningbo Institute of Material Technology and Engineering, Chinese Academy of Sciences, Ningbo, Zhejiang, 315201, China

[c] University of Chinese Academy of Sciences, 100049, Beijing, P. R. China

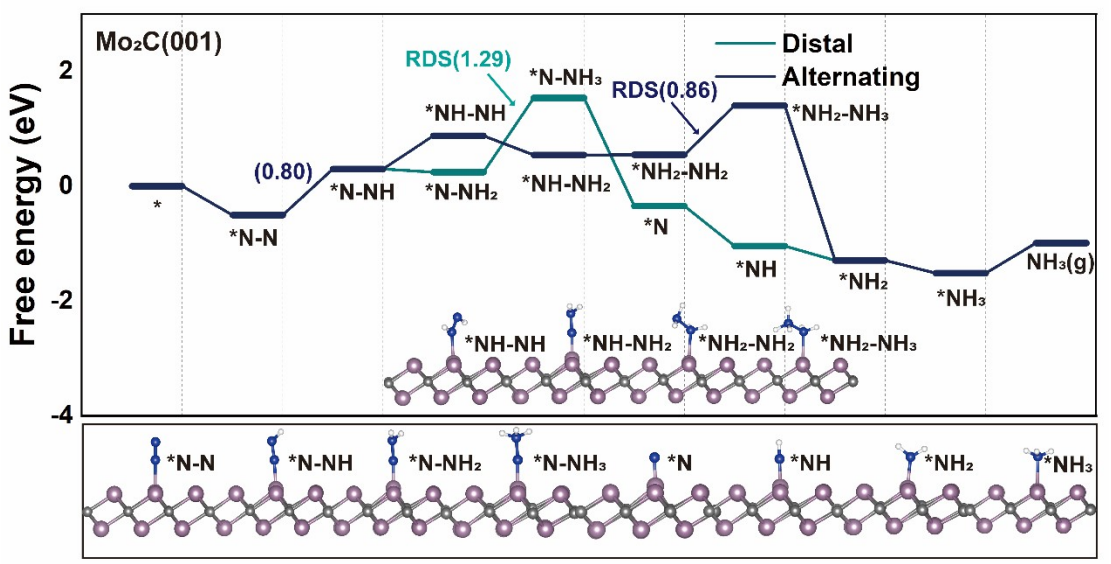

Figure S1 Free energy profile of the N_2 reduction reaction by end-on adsorption on $Mo_2C(001)$ through distal and alternating mechanisms.

Table S1 Computed adsorption energies of N_2 on different TM_A/HMo_2CF_v.

TM	Adsorption energy (eV)		Charge variation * (e)	Charge gain on N_2-end on (e)	Charge gain on N_2-side on (e)
	N_2-end on	N_2-side on			
Ti_A	-0.80	-0.81	+1.39	+1.43	+1.41
V_A	-1.05	-0.05	+1.16	+1.24	+1.15
Cr_A	-1.24	-0.11	+0.89	+0.94	+0.92
Mn_A	-1.33	-0.13	+0.76	+0.82	+0.73
Fe_A	-1.19	-0.02	+0.48	+0.58	+0.54
Co_A	-0.98	0.14	+0.37	+0.51	+0.44
Ni_A	-0.73	-0.75	+0.34	+0.45	+0.44
Mo^{Fv}	-1.14	-0.15	+0.86	+0.90	+1.41
Mo^{Hv}	-1.01		+0.90	+0.99	+0.88

Table S2 Computed adsorption energies of N_2 on different TM_B/HMo_2CF_v.

TM	Adsorption energy (eV)		Charge variation * (e)	Charge gain on N_2-end on (e)	Charge gain on N_2-side on (e)
	N_2-end on	N_2-side on			
Ti_A	-1.13	-0.18	+0.83	+0.96	+0.85
V_A	-1.12	-0.15	+0.85	+0.92	+0.89
Cr_A	-1.10	-0.15	+0.87	+0.95	+0.92
Mn_A	-1.09	-0.16	+0.89	+0.98	+0.95
Fe_A	-1.09	-0.16	+0.91	+0.98	+0.96
Co_A	-1.09	-0.17	+0.93	+0.99	+0.96
Ni_A	-0.75	-0.17	+0.94	+1.05	+0.96
Mo^{Fv}	-1.14	-0.15	+0.86	+0.90	+0.88

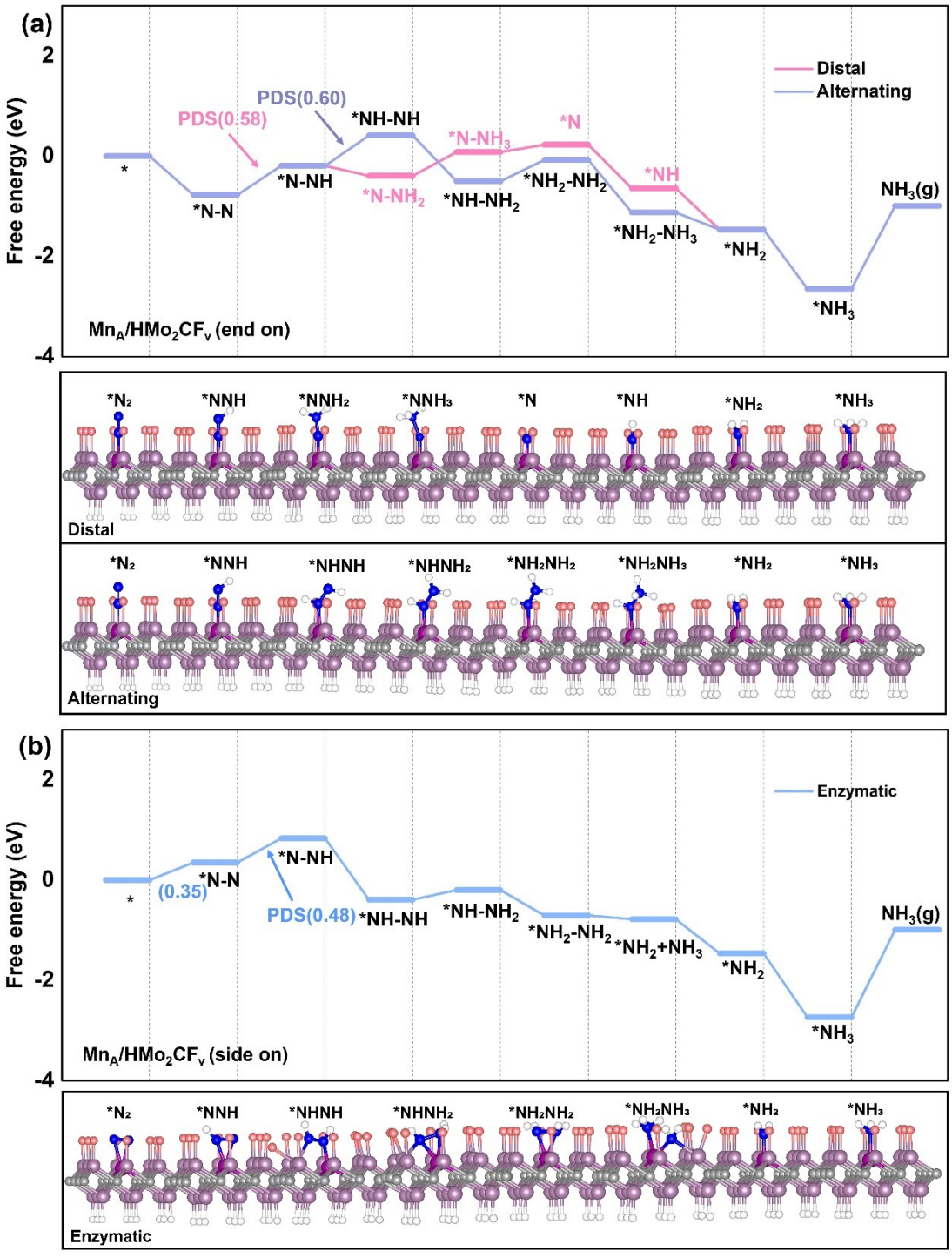

Figure S2 Free energy profile of the N_2 reduction reaction on Mn_A/HMo_2CF_v through (a) distal, alternating, and (b) enzymatic mechanisms.

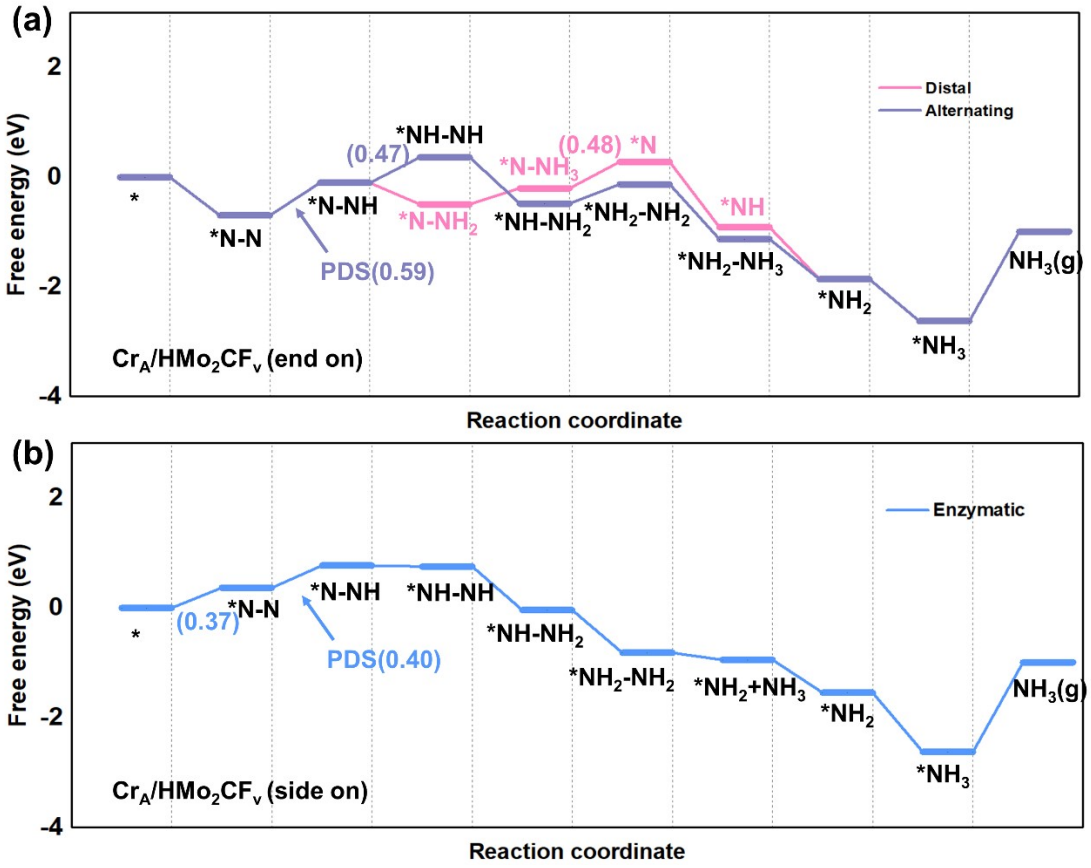

Figure S3 Free energy profile of the N_2 reduction reaction on Cr_A/HMo_2CF_v, through (a) distal, alternating, and (b) enzymatic mechanisms.

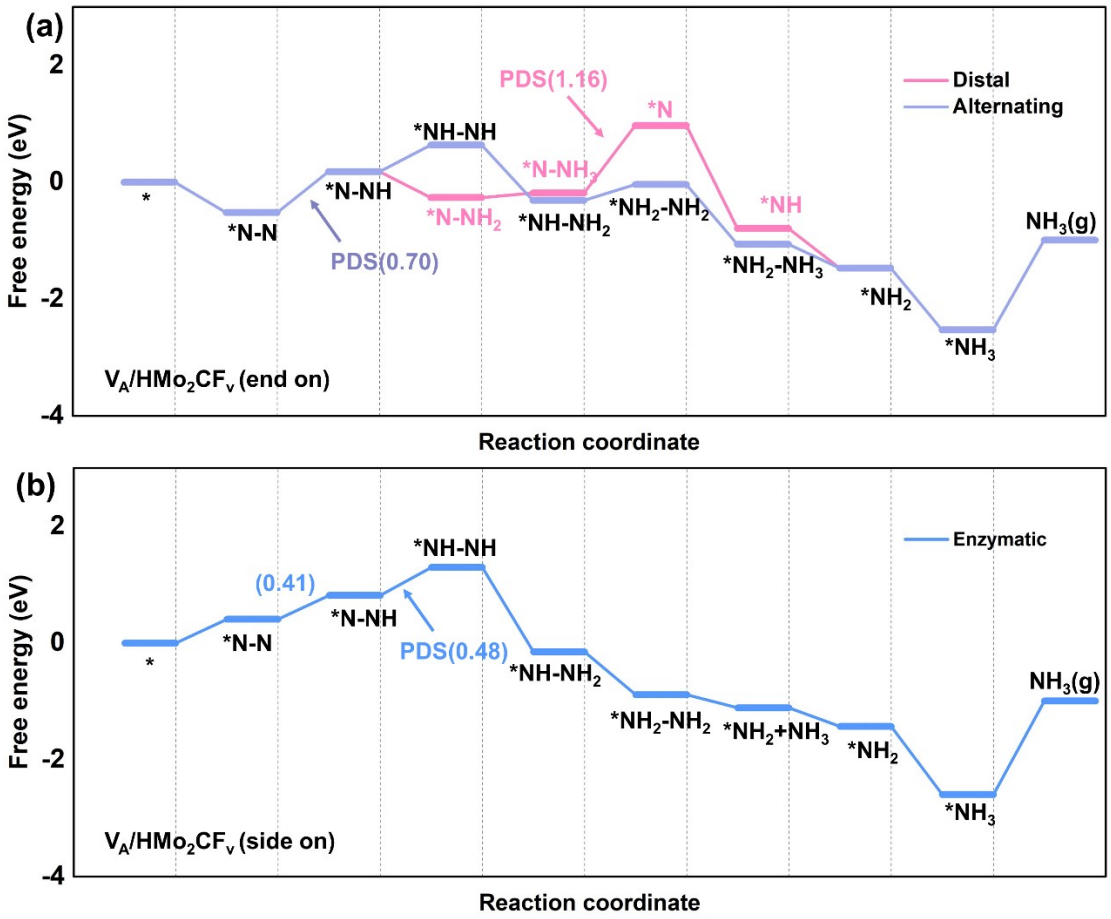

Figure S4 Free energy profile of the N_2 reduction reaction on V_A/HMo_2CF_v through (a) distal, alternating, and (b) enzymatic mechanisms.

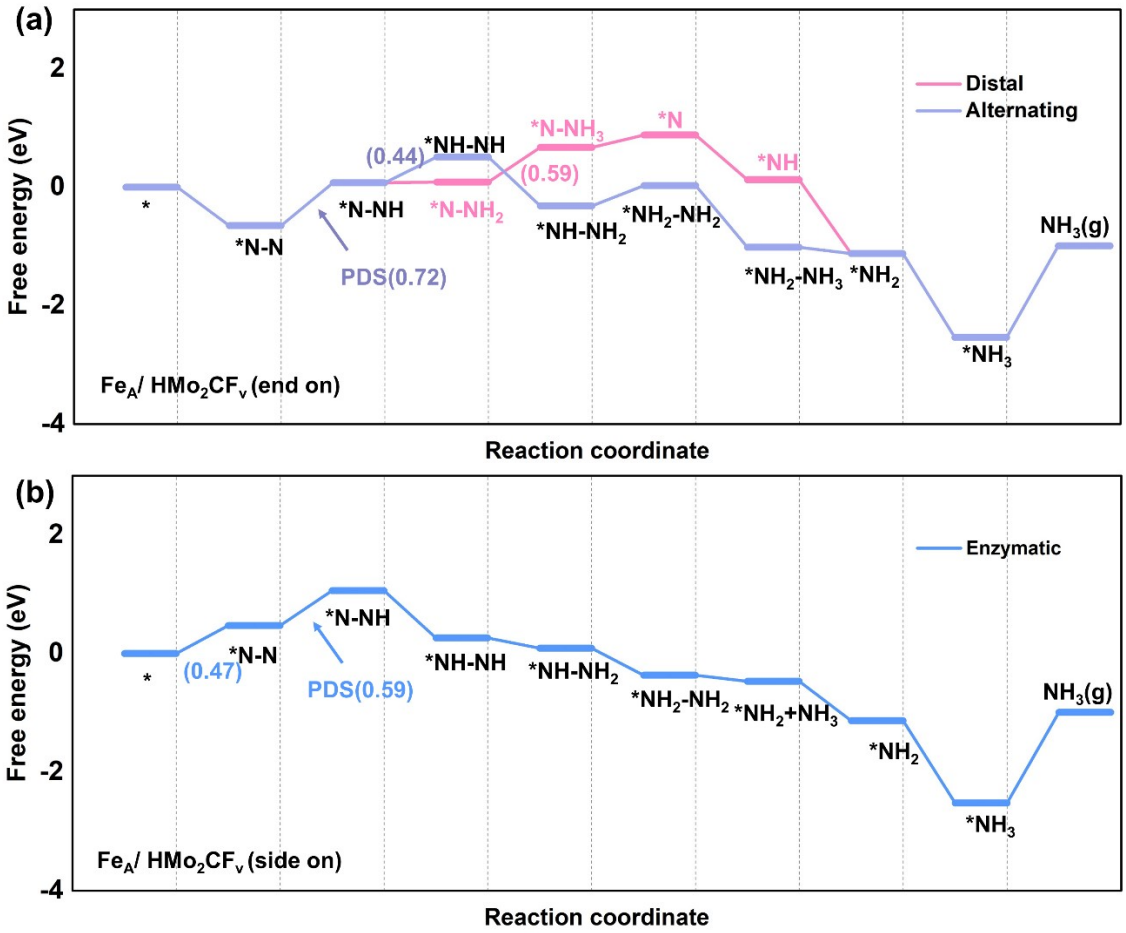

Figure S5 Free energy profile of the N_2 reduction reaction on Fe_A/HMo_2CF_v through (a) distal, alternating, and (b) enzymatic mechanisms.

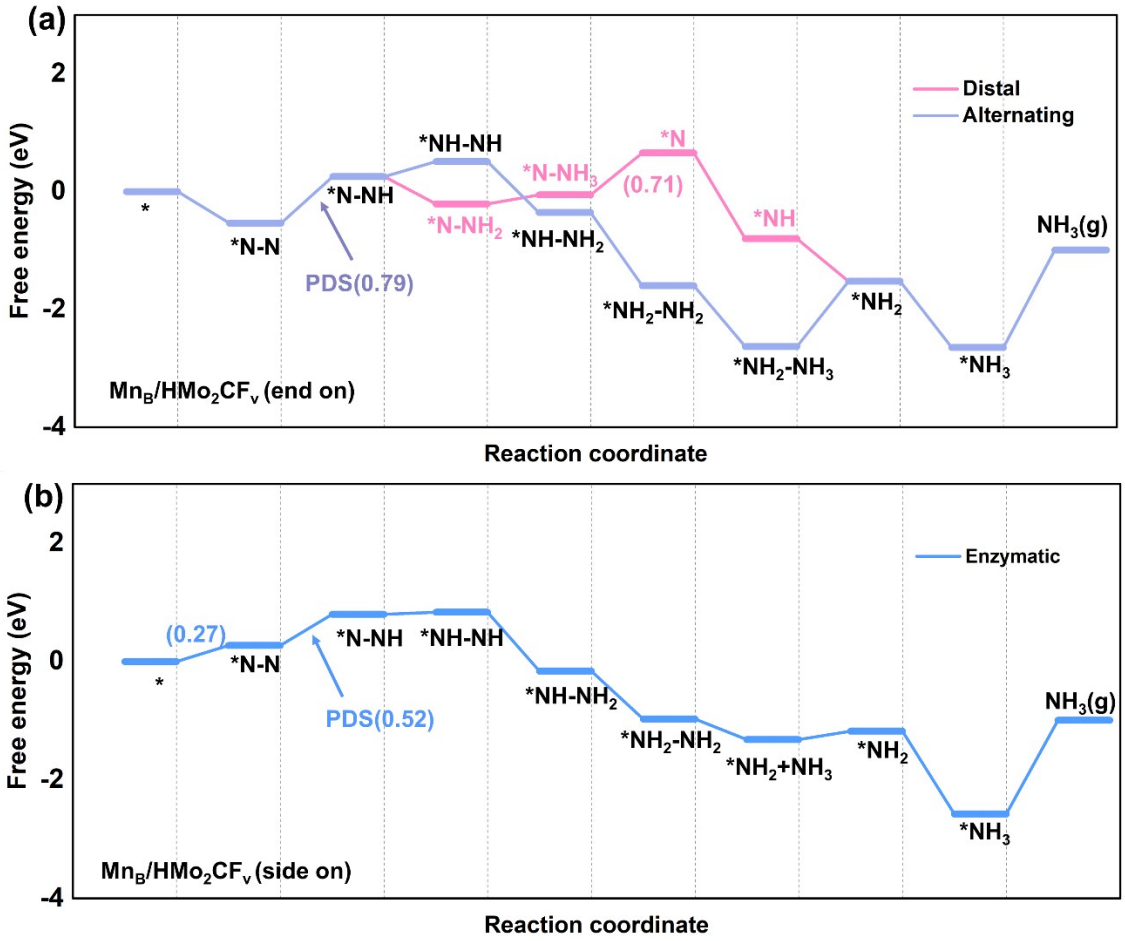

Figure S6 Free energy profile of the N_2 reduction reaction on Mn_B/HMo_2CF_v through (a) distal, alternating, and (b) enzymatic mechanisms.

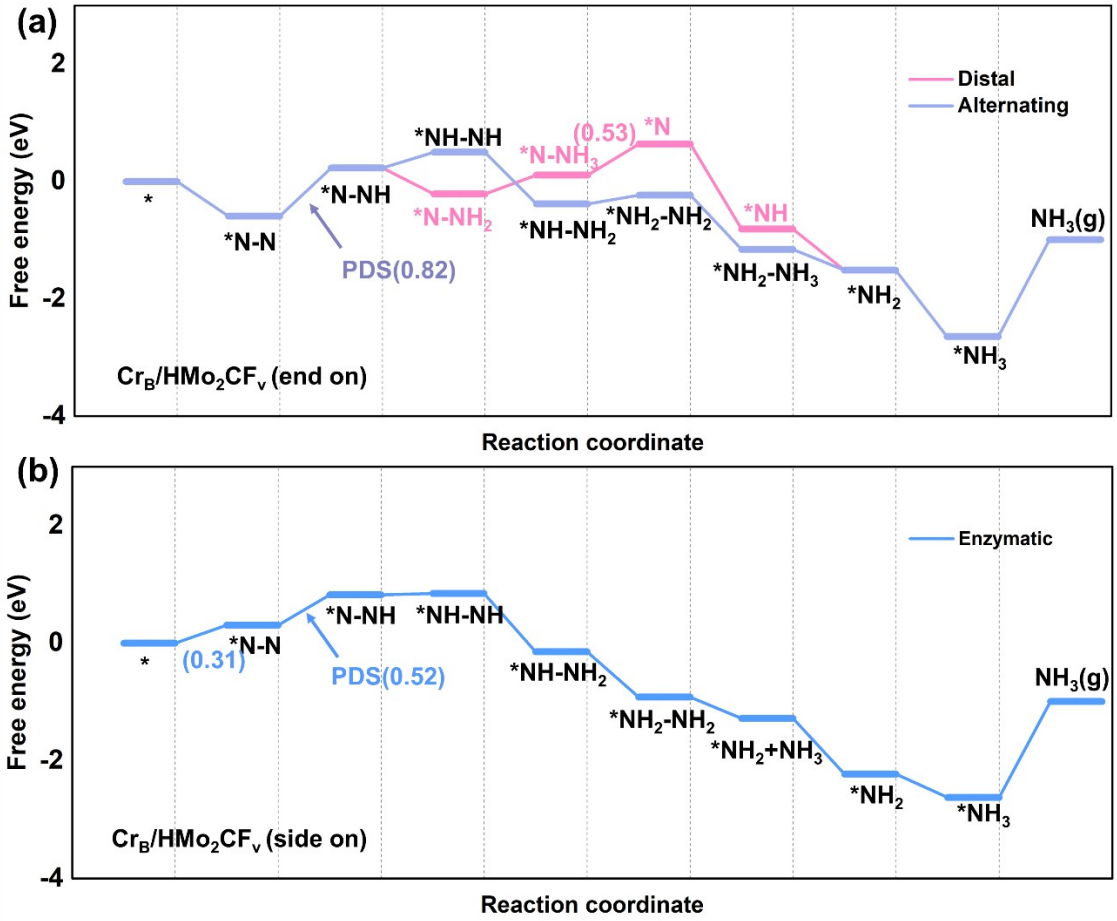

Figure S7 Free energy profile of the N_2 reduction reaction on Cr_B/HMo_2CF_v through (a) distal, alternating, and (b) enzymatic mechanisms.

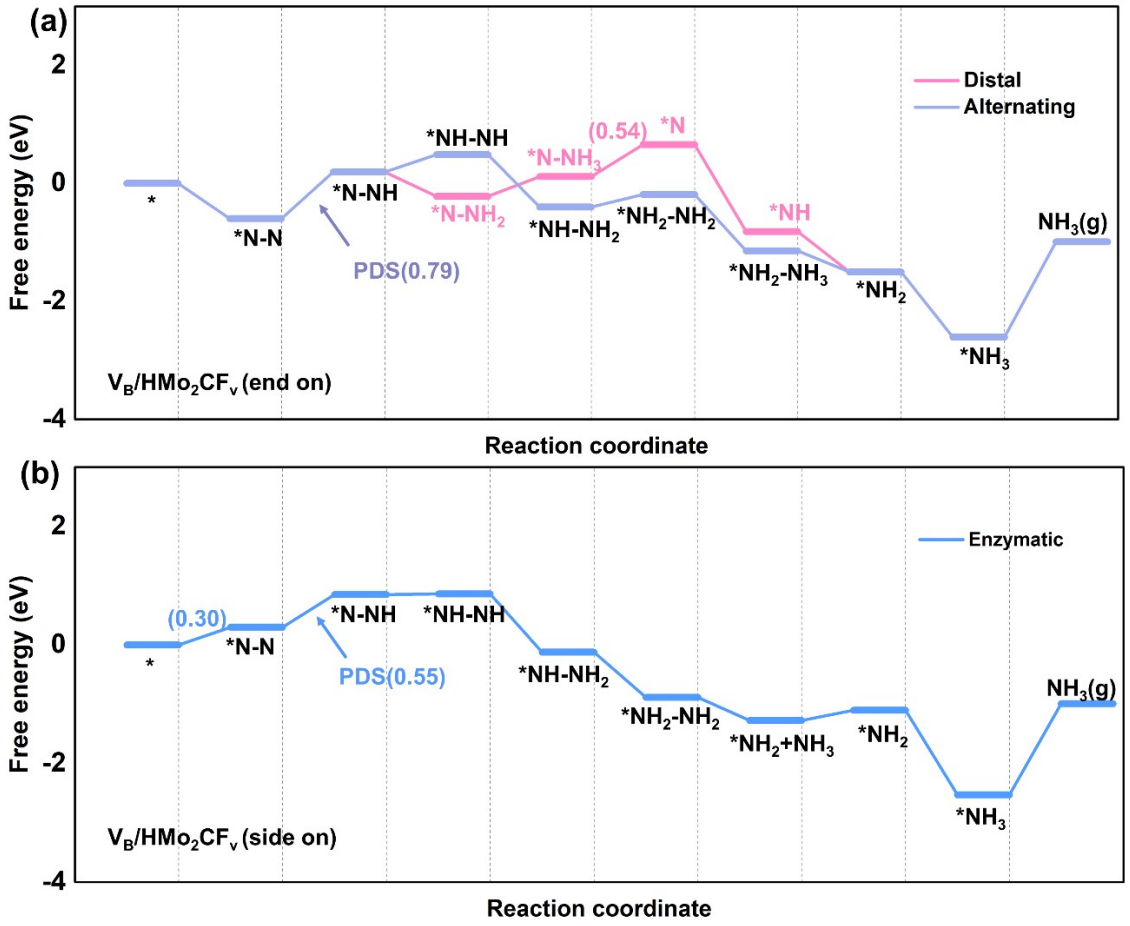

Figure S8 Free energy profile of the N_2 reduction reaction on V_B/HMo_2CF_v through (a) distal, alternating, and (b) enzymatic mechanisms.

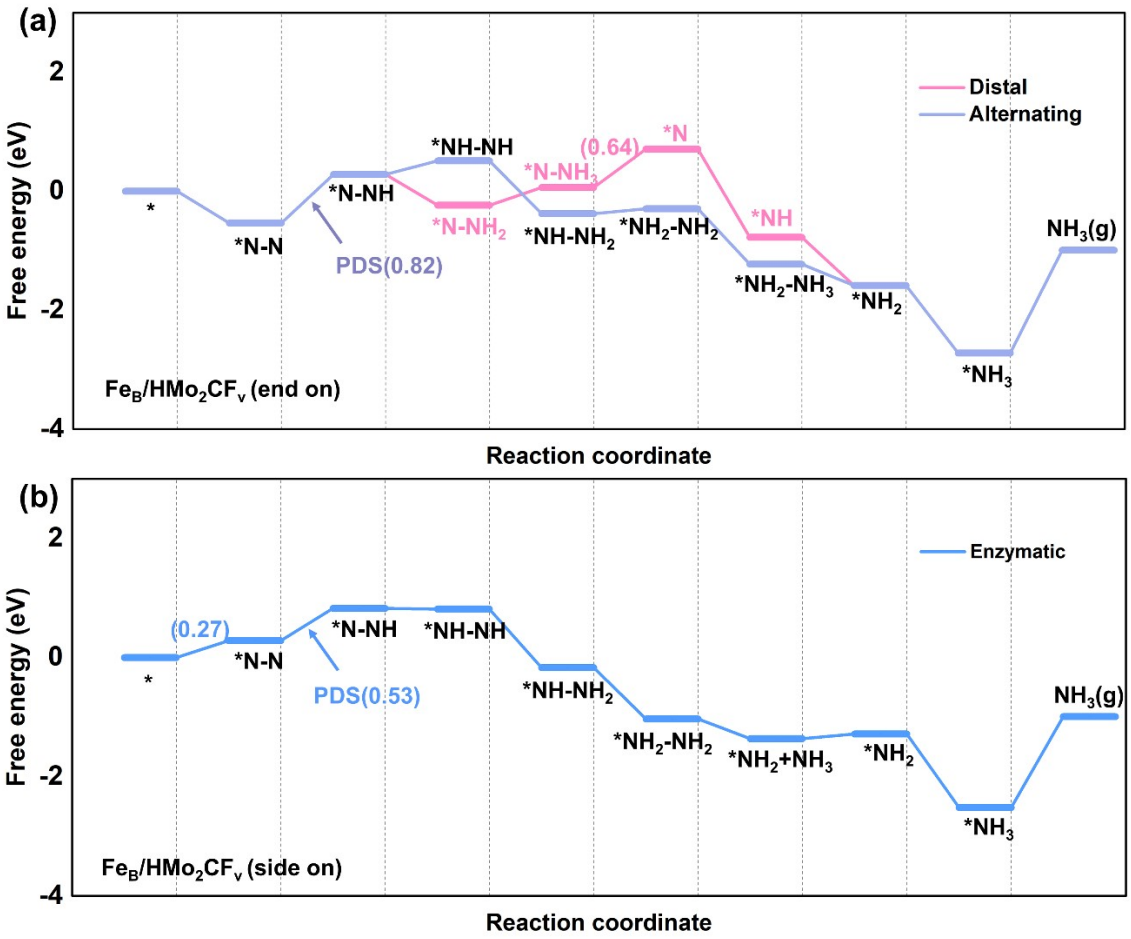

Figure S9 Free energy profile of the N_2 reduction reaction on Fe_B/HMo_2CF_v through (a) distal, alternating, and (b) enzymatic mechanisms.

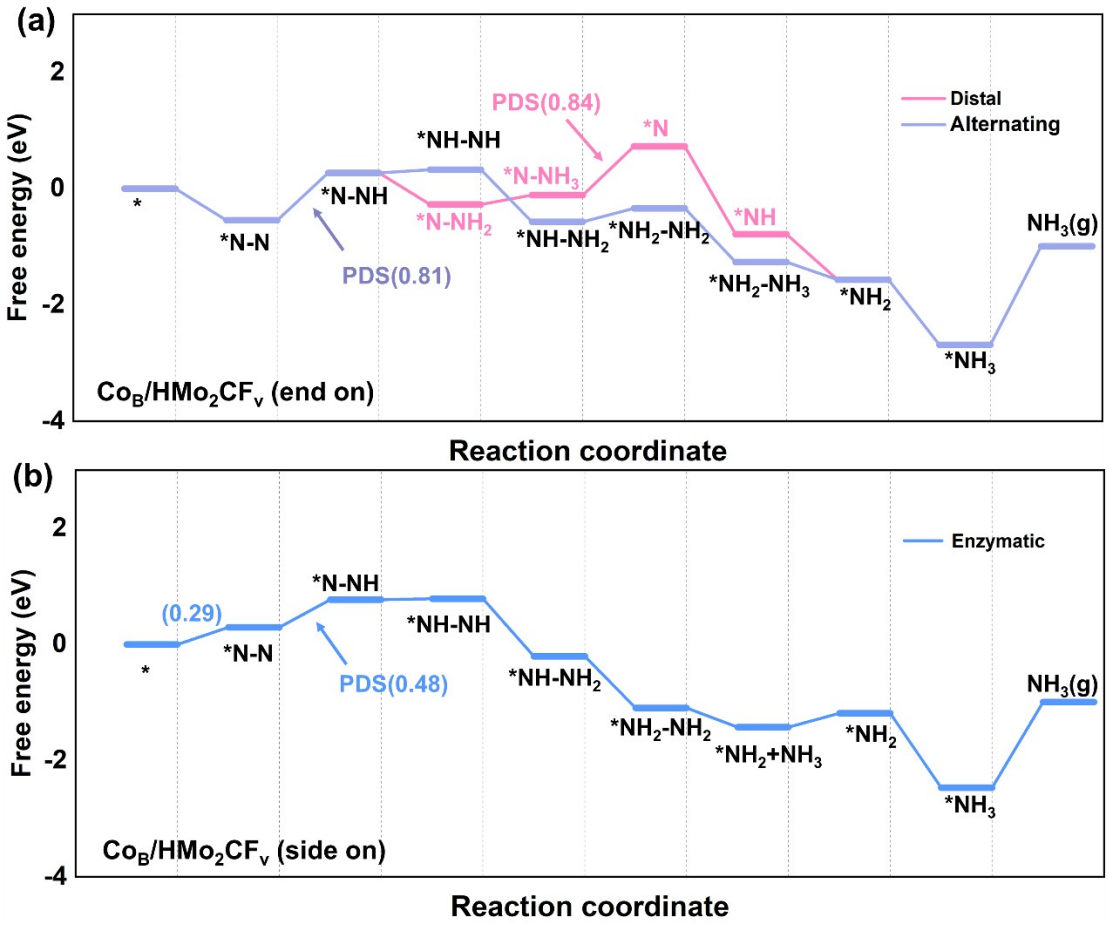

Figure S10 Free energy profile of the N_2 reduction reaction on Co_B/HMo_2CF_v through (a) distal, alternating, and (b) enzymatic mechanisms.

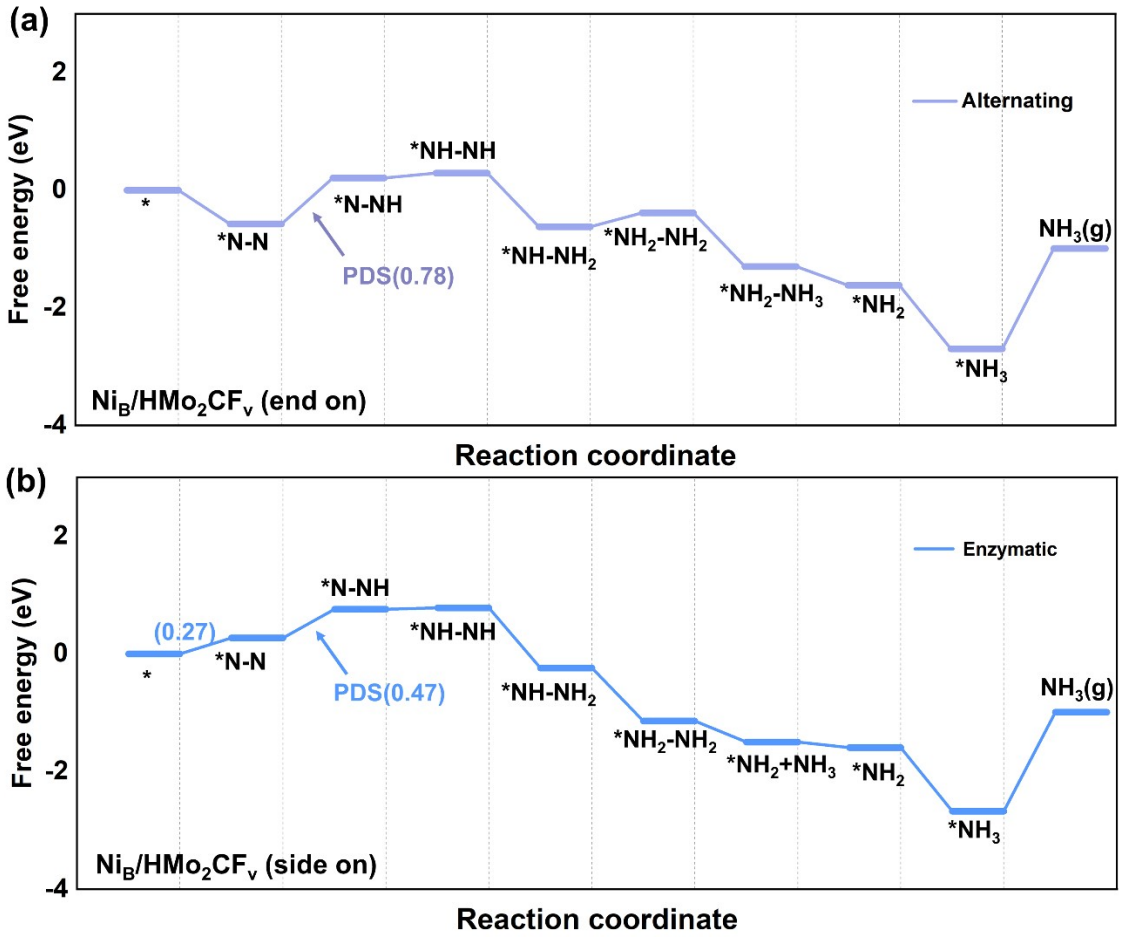

Figure S11 Free energy profile of the N_2 reduction reaction on Ni_B/HMo_2CF_v through (a) alternating, and (b) enzymatic mechanisms.

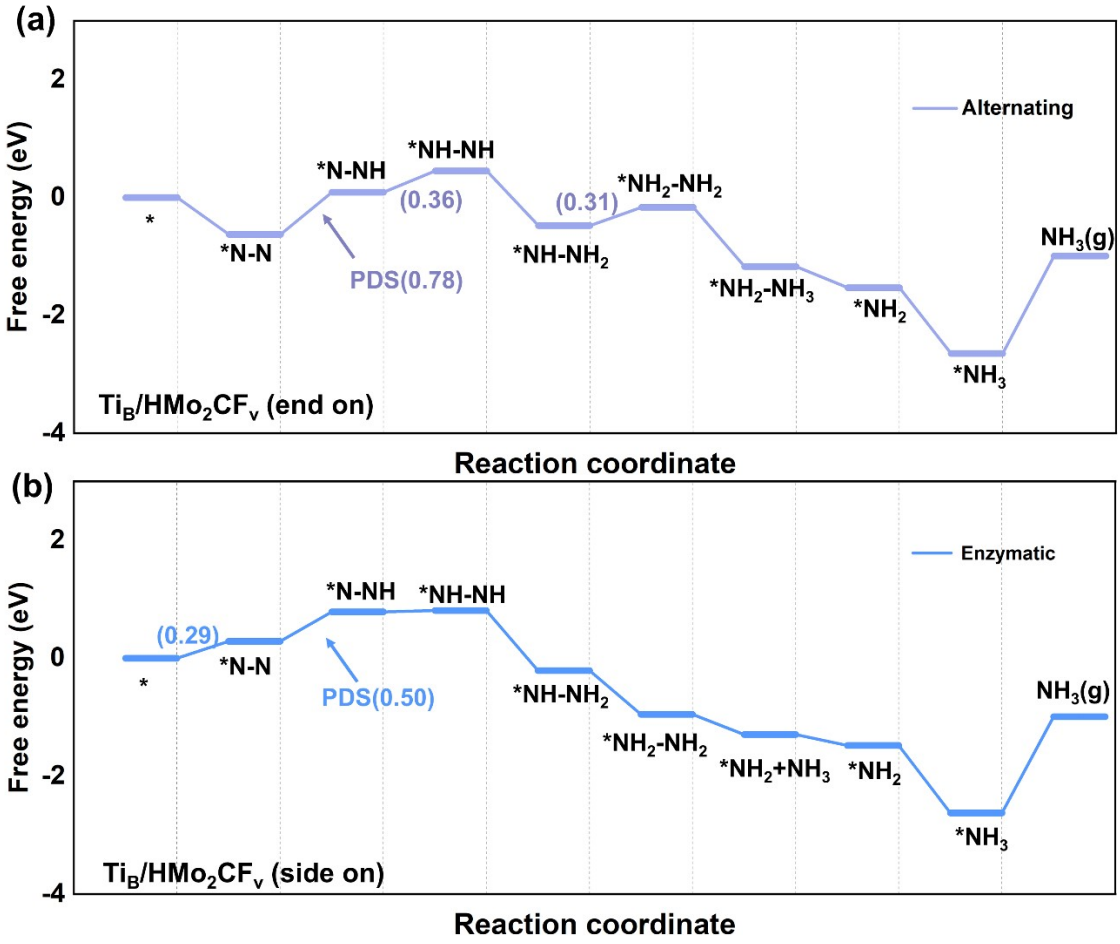

Figure S12 Free energy profile of the N_2 reduction reaction on Ti_B/HMo_2CF_v through (a) alternating, and (b) enzymatic mechanisms.

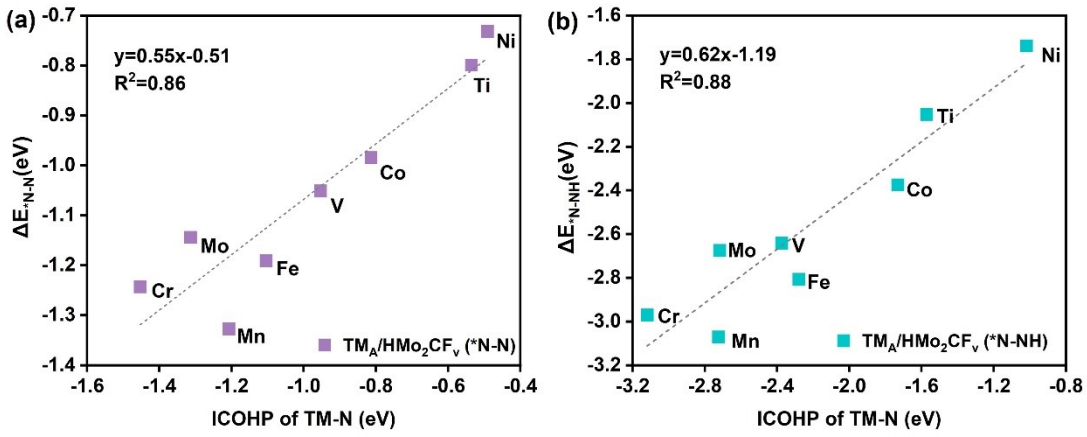

Figure S13 The linear correlation relationship between ICOHP of TM-N and ΔE (*N-N) for TM_A/HMo_2CF_v (a) ICOHP of TM-N and ΔE (*N-NH) for TM_A/HMo_2CF_v (b).